Citation: Molecular Therapy — Methods & Clinical Development (2016) **3,** 16031; doi:10.1038/mtm.2016.31
Official journal of the American Society of Gene & Cell Therapy
www.nature.com/mtm

ARTICLE

A scalable method for the production of high-titer and high-quality adeno-associated type 9 vectors using the HSV platform

Laura Adamson-Small[1], Mark Potter[1], Darin J Falk[2], Brian Cleaver[1], Barry J Byrne[1] and Nathalie Clément[1]

Recombinant adeno-associated vectors based on serotype 9 (rAAV9) have demonstrated highly effective gene transfer in multiple animal models of muscular dystrophies and other neurological indications. Current limitations in vector production and purification have hampered widespread implementation of clinical candidate vectors, particularly when systemic administration is considered. In this study, we describe a complete herpes simplex virus (HSV)-based production and purification process capable of generating greater than 1×10^{14} rAAV9 vector genomes per 10-layer CellSTACK of HEK 293 producer cells, or greater than 1×10^{5} vector genome per cell, in a final, fully purified product. This represents a 5- to 10-fold increase over transfection-based methods. In addition, rAAV vectors produced by this method demonstrated improved biological characteristics when compared to transfection-based production, including increased infectivity as shown by higher transducing unit-to-vector genome ratios and decreased total capsid protein amounts, shown by lower empty-to-full ratios. Together, this data establishes a significant improvement in both rAAV9 yields and vector quality. Further, the method can be readily adapted to large-scale good laboratory practice (GLP) and good manufacturing practice (GMP) production of rAAV9 vectors to enable preclinical and clinical studies and provide a platform to build on toward late-phases and commercial production.

Molecular Therapy — Methods & Clinical Development (2016) **3**, 16031; doi:10.1038/mtm.2016.31; published online 11 May 2016

INTRODUCTION

The unmatched capability of recombinant adeno-associated vectors (rAAV) to convey robust and long-term gene expression in a wide array of target tissues has triggered a multitude of preclinical as well as clinical studies enabling successful gene transfer for human genetic diseases. As a direct consequence, the requirement for very high amounts of high quality rAAV stocks has greatly increased and underscored the limitations of current production systems (recently reviewed in ref. 1). This holds specifically true for the treatment of inherited genetic diseases such as muscular dystrophies, when body-wide gene transfer may be required, relying on systemic dosing often at high AAV doses.[2–5]

Gene transfer protocols for Pompe disease, Duchenne muscular dystrophy (DMD), and spinal muscular atrophy are among the most advanced for neuro-muscular disorders, with a plethora of preclinical data and a few clinical trials[3,5–9] Among the various AAV serotypes used in these studies, AAV9 has emerged as one of the most powerful serotype for its widespread cardiac and skeletal muscle transduction,[10–12] as well as the ability to cross the blood–brain barrier and lead to central nervous system transduction,[13–15] also a key target in neurodegenerative disease following systemic delivery.[16–19]

Previous studies of rAAV in clinical trials for muscular dystrophy have delivered vector via intramuscular injection often due to the lack of large-scale manufacturing capabilities to generate the amounts needed to support systemic administration.[6] Additionally, preclinical studies initiated over the past few years have required an unprecedented amount of AAV vectors for studies in larger species to enable complete toxicology and bio-distribution studies to model predicted dosing humans. Current vector requirements for clinical studies suggest doses in excess of 1×10^{14} vg/kg, or $> 4\times10^{15}$ vector genomes (vg) for a single 10-kg subject, in a single rAAV dose.[20] As a result, rAAV amounts exceeding 1×10^{16} to 1×10^{17} vg have become a common request to good laboratory practice (GLP) and good manufacturing practice (GMP) manufacturing facilities. With the currently available processes, supporting such scale remains a critical challenge for most if not all laboratories. As the use of rAAV expands, the development of more efficient and scalable methods is essential.

Although rAAV is one of the most straightforward viruses to produce *in vitro* due to the relative simplicity of its life cycle and genome design, it has been difficult to provide solutions for a streamline large-scale production and purification method. To date, four production methods have been implemented for the manufacture of clinical AAV products (recently reviewed in ref. 1): transfection,[21–23] packaging cell lines with adenovirus infection,[24] baculovirus expression system,[25–28] and the herpes virus system (HSV).[29–32] It is widely accepted that transfection protocols relying on adherent cell platforms are not suitable for large scale-up purposes due to their intrinsic lack of scalability. Transfection and infection protocols using suspension cell culture present obvious advantages related to scalability. Yields as high as 1×10^{5} vg/cell, or 1×10^{14} vg/l of cell culture have been reported

[1]Department of Pediatrics, Powell Gene Therapy Center, University of Florida, Gainesville, Florida, USA; [2]Department of Pediatrics, Child Health Research Institute, University of Florida, Gainesville, Florida, USA. Correspondence: BJ Byrne (bbyrne@ufl.edu) Or N Clément (nclement@peds.ufl.edu)
Received 22 March 2016; accepted 28 March 2016

for these methods.[21,26,28,31–33] However, the yields often reflect the amount in crude lysates prior to virus purification and are often intrinsically correlated to the higher cell density reachable in suspension. More importantly, to date, no production system for AAV9 has been described resulting in high particle yield with superior potency. To the contrary, baculovirus-generated AAV products have often demonstrated reduced infectivity when compared to transfection-generated material.[25,27,34,35]

The production system using HSV as a shuttle virus to deliver all AAV cis- and trans-functions to support replication and packing in producer cells was originally developed by our group[29,30] in an adherent format using HEK 293 cells. Byrne and colleagues demonstrated that coinfection of HEK 293 with two recombinant HSV engineered to carry the rAAV vector genome or the AAV helper functions, Rep and Cap ORFs, resulted in successful AAV packaging. This approach was then further modified, to support large-scale AAV production using a suspension-adapted BHK cells format.[32] The system has been transferred to a GMP setting for the clinical manufacturing of an AAV1 product currently in use in clinical trials.[36]

To date, a method specifically designed and optimized for the production of high-titer, high-potency clinical grade rAAV9 is lacking. The work presented here is focused on the development of an HSV-based production method specifically designed for rAAV9 as a platform amenable to large-scale preclinical and clinical studies. The upstream production methodology is used with a novel purification process previously described by our group which permits efficient recovery of infectious rAAV9 material.[37] Here, we report the production and purification of rAAV9 preparations greater than 10^{14} vector genomes per CS10 in a final product formulated for preclinical and clinical applications.

This method is likely extendable to other serotypes and should bridge the gap between preclinical research, early phase clinical studies, and large-scale, worldwide development of gene therapy based-drugs for genetic diseases and disorders.

RESULTS

Recombinant HSV stocks production and characterization

Two recombinant HSV constructs were utilized for this study: rHSV-GFP (aka rHSV-UF5), that contains the AAV genome carrying the AAV2 ITRs, the CMV promoter driving the expression of a humanized GFP,[29] and rHSV-AAV2/9 that contains the AAV packaging functions, AAV2 Rep and AAV9 Cap sequences under the control of the AAV2 P5 promoter (Figure 1). Recombinant HSV stocks were produced in V27 cells, a Vero derivative cell line that contains a stable expression cassette for HSV Infected Cell Protein 27 (ICP27) using the 10-layers CellSTACKs (abbreviated CS10) culture system. Final filtered stocks were titered by a traditional plaque assay. The average yield per CS10 was 4.58×10^{10} plaque forming unit (PFU)/CS10 $\pm 2.19\times10^{10}$ (n=4) for rHSV-GFP and an average of 3.85×10^{10} PFU/CS10 $\pm 9.32\times10^{9}$ (n = 4) for rHSV-AAV2/9 with no significant difference detected between the construct and the helper stocks. The average PFU/cell ranged between 80 and 100, which was consistent with previously reported titers for other rHSV constructs.[38] Our data also showed a recovery in excess of 90% of the HSV viral input upon concentration by tangential flow filtration. A subset of HSV stocks were stored frozen for a period exceeding 12 months and did not exhibit a loss of infectivity (data not shown).

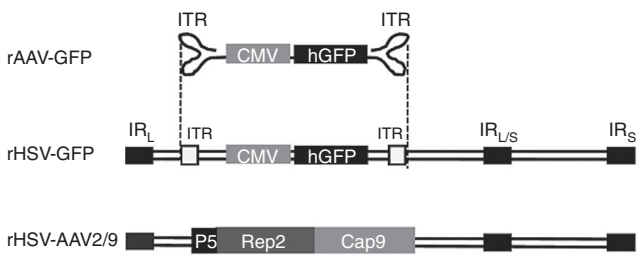

Figure 1 Schematic representation of recombinant adeno-associated virus (rAAV) and rHSV constructs. Not to scale. CMV, cytomegalovirus promoter; hGFP, humanized green fluorescent protein; ITR, AAV2 inverted terminal repeats; IR$_{L/S}$, HSV inverted repeat long/short.

Process optimization for rAAV9 production at small-scale

Preliminary process optimization was performed at small-scale using HEK 293 cells in T225 cell culture flasks. Cells were seeded 24 hours prior to infection, and one flask was used for each experiment to determine the exact cell number at the time of infection in order to calculate the amount of each HSV to be used. Various parameters that may impact the kinetics and efficacy of HSV infection as well as rAAV packaging, were evaluated side-by-side including: multiplicity of infection (MOI) with each rHSV, incubation times with the HSV-containing inoculum, infection in the presence or absence of fetal bovine serum, and harvest time points. Yields were assessed based on the transducing unit titers in crude, Benzonase-treated and clarified cell lysates. Optimal coinfection conditions were found to be using a MOI of 2 and 12 with rHSV-GFP and rHSV-AAV2/9 respectively, with an inoculum performed in a serum-containing medium for a period of 48–55 hours postinfection, or time of harvest, resulting in an average of $6.54\times10^{8}\pm2.06\times10^{8}$ TU per flask (n = 7). Higher MOIs of the helper rHSV resulted in saturation of the total rAAV9 output, while lower MOIs resulted in lower rAAV9 yields. These results were in line with results reported by others for alternative serotypes.[32] Shorter incubation times of the HSV-containing inoculum (2 to 6 hours) in the presence or absence of serum, followed by medium change, consistently resulted in a reduced yield from two- to fivefold. It was also observed that the total AAV output was proportional to the total number of cells at time of infection and that supra-confluent cells could be infected efficiently.

Optimal coinfection conditions were used to compare HSV-mediated rAAV9-GFP yields to transfection-generated yields in T225 flasks. Coinfected cells were assayed side-by-side with transfected cells using our standard cotransfection protocol.[37] The two plasmids used for transfection were the closest in design to the rHSV constructs: plasmid pTR-UF5 containing the AAV genome with a humanized GFP downstream of the CMV promoter was used to create rHSV-GFP; pDG-UF9-KanR (helper) contained the same AAV2/9 cassette as used in the rHSV-UF9 construct with the exception of the P5 promoter that has been replaced by the MMTV promoter, similar to the parental pDG plasmid.[22] Results revealed about a 10-fold increase in rAAV9-GFP in transducing units from HSV infected cells when compared to transfected cells based on transducing unit titers with an average $6.66\times10^{7}\pm4.43\times10^{7}$ TU (n = 6) in transfection lysates.

Large-scale production of rAAV9 using GMP process-similar methods and comparison to transfection protocol

We next scaled-up the infection protocol and combined it with a robust purification method to generate highly pure rAAV9-GFP stocks. Over the past few years, our group has acquired extensive data related to rAAV9 production for both GLP and GMP-grade rAAV9 for preclinical and clinical studies. Our protocol was based on calcium phosphate ($CaPO_4$) transfection of HEK 293 cells in CellSTACKs, followed by one-step column chromatography purification and

concentration by tangential flow filtration[37] (Figure 2a). In this study, our goal was to thoroughly compare the yield and quality of the vector generated by rHSV coinfection side-by-side with transfection-derived AAV9 (Figure 2a).

Upstream production steps were performed in a similar fashion for each single experiment with the following differences, intrinsic to the method chosen: for transfection, cell confluence was between 60–70% (average 6.44×10^8 cells, $n = 3$) at time of transfection to ensure optimal transfection efficacy; for infection, cells were infected at higher confluence ranging between 70 to 100% (average 8.07×10^8 cells, $n = 3$). The $CaPO_4$/DNA precipitate was left on the cells for approximately 72 hours while the HSV inoculum was incubated for 48–52 hours as previously discussed. Cells were harvested by standard procedure using 5 mmol/l ethylenediaminetetraacetic acid (EDTA) to detach the cells from transfection. Infected cells were readily detachable by shaking the flasks. Cells were washed in phosphate buffer saline (PBS) and pelleted by centrifugation. Each pellet weight was carefully measured as the starting material for the purification steps. Downstream purification and concentration processes were performed identically and independently of the production method used (Figure 2b,c).[37]

Final concentrated vector stocks were assessed for vector genome titers using three independent methods, including standard quantitative real-time polymerase chain reaction (qPCR), digital droplet PCR (ddPCR), and Dot Blot in view of bridging our data across assays. The current lack of a standardized method for rAAV vector genome quantification and infectious units limits the ability to compare true vector yield across laboratories. By using three of the preferred methods for the quantification of rAAV vector genome, we aimed to provide a small yet thorough comparative quantification across these methods while providing the reader with a reference to their method of choice. The titer variability between these three methods was less than 35% for each preparation assessed. Importantly, the three methods exhibited high similarity with regards to the yields obtained for each production methods (Figure 3a). For the sake of clarity, our standard Q-PCR assay was used to assess overall production system performance for the rest of the study. The overall vector genome titers were

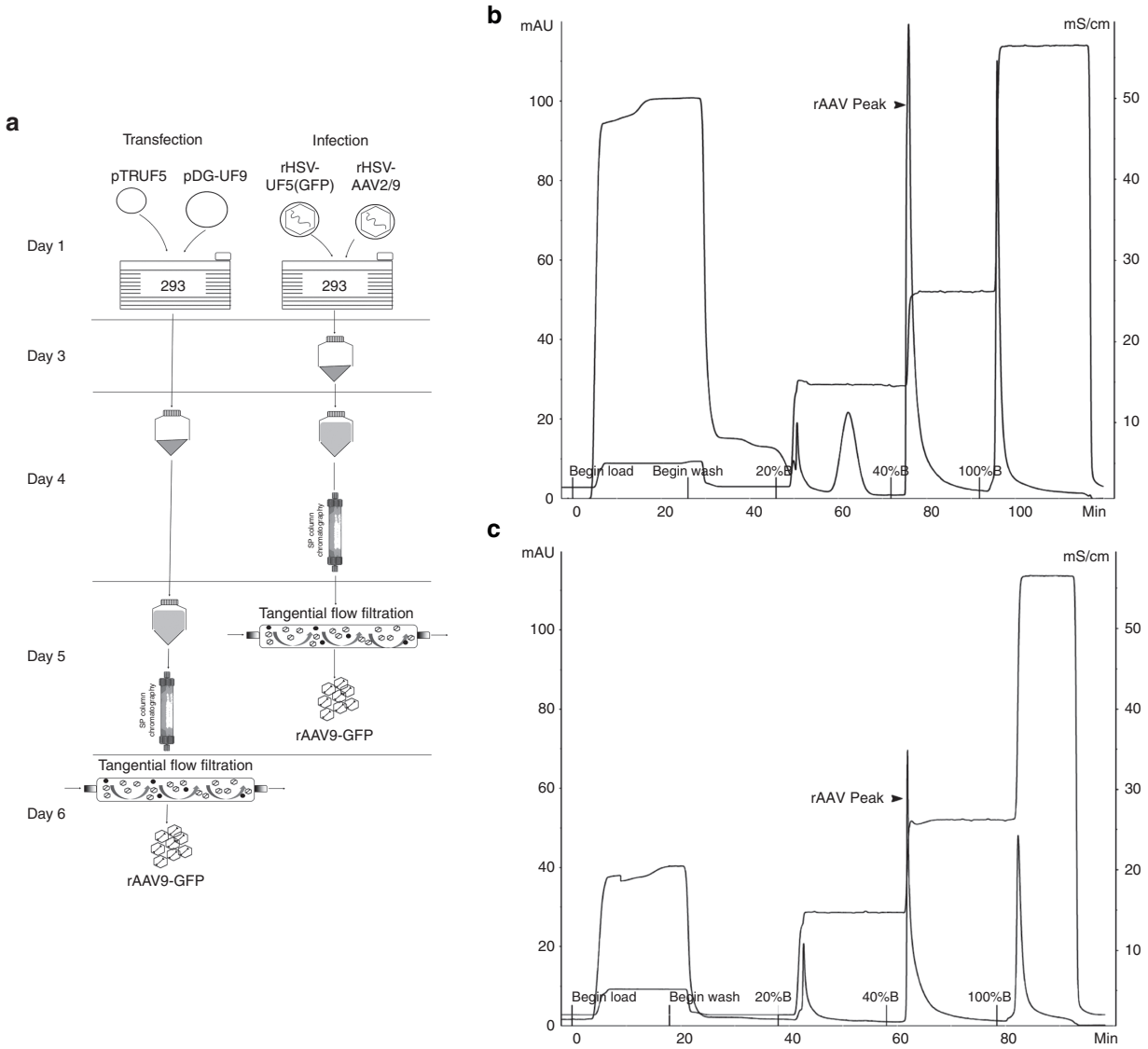

Figure 2 Large-scale adeno-associated virus-9 production and purification processes. (**a**) Schematic representation of transfection and infection production method and purification processes. Anion-exchange chromatography by SP column and concentration Tangential Flow filtration are depicted. (**b** and **c**) Chromatography chromatograms. Representative chromatogram for Opt. infection (**b**) of transfection (**c**) are shown. UV signal (peak line) and conductivity (step line) are shown. First step is 20% B, second step or elution step is 40% B and last step is 100% B.

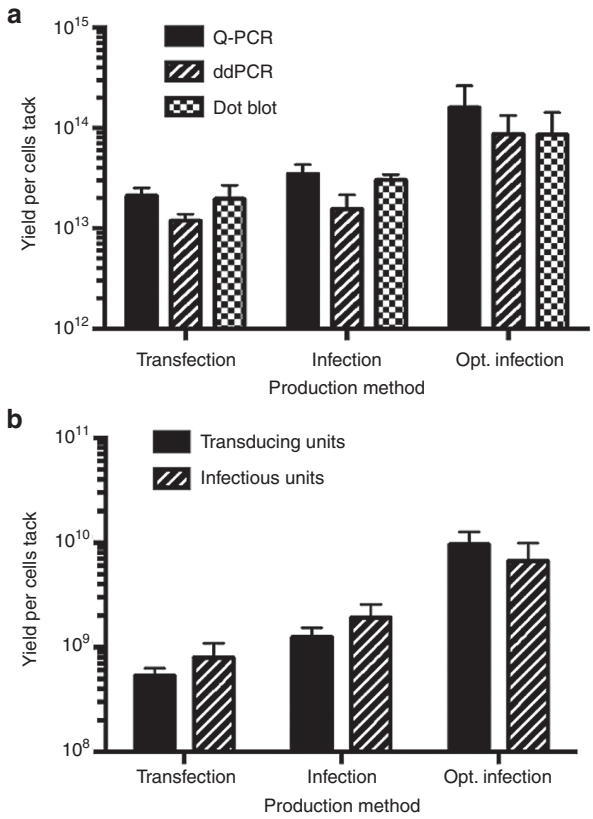

Figure 3 Large-scale adeno-associated virus (AAV)9 yields by transfection or HSV-infection. Average and standard deviation for each production method: transfection ($n = 4$ independent production runs), infection ($n = 3$), and optimized (Opt.) infection ($n = 2$). For each quantification methods, titers were obtained from two to three independent assays and average for each AAV9 preparation. (**a**) Vector genomes. Total AAV9 Benzonase-resistant vector genome yields per CS10 are shown from three different quantification methods. ddPCR, digital droplet polymerase chain reaction; Q-PCR, quantitative real-time PCR. (**b**) Infectious units. Total transducing or infectious unit per CS10 shown for each production method.

significantly increased by ~64% when using the coinfection method compared to the transfection method with a final average yield of 3.47×10^{13} vg per CS10 ($P < 0.05$; Figure 3a and Table 1). The average yield of 2.11×10^{13} vg per CS10 from transfected cells was in line with historic yields obtained for other constructs using the same method, typically ranging between 1 and 2×10^{13} vg/CS10. Based on cell counts at the time of infection or transfection, the yield per cell obtained from infection (4.42×10^4 vg/cell) was slightly higher than the one obtained for transfection (3.27×10^4 vg/cell), that, in combination with the higher cell numbers, resulted in the observed yield increase. We next expressed the vector yield per the cell mass obtained at the time of harvest. Direct cell counting is challenging at this step due to a damaged cellular phenotype. Interestingly, this measure revealed a significant difference between HSV and plasmid generated rAAV with an almost threefold increase of the vg/mg as compared to transfection results ($P < 0.01$; Table 1). A possible explanation may be related to the shorter incubation time for the infected cells (48 hours) as compared to 72 hours for the transfected cells, reducing the time for cell division. Pellet weights for HSV-mediated production were on average 44% (1.8-fold) smaller than those obtained by transfection.

The amount of free rAAV9-GFP present in the supernatant was assessed in several infection experiments by direct transducing assay without any further sample processing. We consistently observed

Table 1 *In vitro* characteristics of rAAV9-GFP made by transfection or HSV infection-based methods

	Transfection	*Infection*	*Optimized infection*
Yield (VG/CS)	$2.11 \times 10^{13} \pm 3.97 \times 10^{12}$	$3.47 \times 10^{13} \pm 8.12 \times 10^{12}$	$1.59 \times 10^{14} \pm 1.04 \times 10^{14}$
Yield (TU/CS)	$5.29 \times 10^{8} \pm 9.67 \times 10^{7}$	$1.24 \times 10^{9} \pm 2.86 \times 10^{8}$	$9.54 \times 10^{9} \pm 3.02 \times 10^{9}$
Yield (IU/CS)	$7.98 \times 10^{8} \pm 2.93 \times 10^{8}$	$1.92 \times 10^{9} \pm 6.51 \times 10^{8}$	$6.66 \times 10^{9} \pm 3.23 \times 10^{9}$
VG/cell	$3.27 \times 10^{4} \pm 6.17 \times 10^{3}$	$4.42 \times 10^{4} \pm 1.17 \times 10^{4}$	$1.08 \times 10^{5} \pm 7.17 \times 10^{4}$
TU/cell	0.82 ± 0.15	1.64 ± 0.74	6.44 ± 2.13
Ratio VG:TU	$4.13 \times 10^{4} \pm 1.28 \times 10^{4}$	$2.84 \times 10^{4} \pm 5.82 \times 10^{3}$	$1.58 \times 10^{4} \pm 5.94 \times 10^{3}$
Pellet (mgs/CS)	$9.40 \times 10^{3} \pm 1.21 \times 10^{3}$	$5.30 \times 10^{3} \pm 3.61 \times 10^{2}$	$1.14 \times 10^{4} \pm 8.49 \times 10^{2}$
VG/mgs	$2.24 \times 10^{9} \pm 3.68 \times 10^{8}$	$6.63 \times 10^{9} \pm 2.02 \times 10^{9}$	$1.37 \times 10^{10} \pm 8.11 \times 10^{9}$
AUC (mAU*min)	96.04 ± 14.72	117.42 ± 31.03	208.94 ± 16.49
% Full	16.46 ± 6.43	N/A	27.81 ± 1.12
Purity (%)	94.05 ± 2.17	98.10 ± 1.61	99.55 ± 0.64
rHSV (PFU/ml)	N/A	< 100 PFU/ml	< 100 PFU/ml

Average and standard deviation are shown. Transfection ($n = 4$); infection ($n = 3$); optimized (Opt.) infection ($n = 2$), except for % full (obtained by electron-microscopy): ($n = 2$) each.

AAV, adeno-associated virus; AUC, area under the curve; CS10, Cellstack; HSV, herpes simplex virus; IU, infectious unit; N/A, not applicable; PFU, plaque forming unit; TU, transducing unit; Unicorn Software, GE Healthcare; VG, vector genome.

*Significantly different from transfection values, $P < 0.05$.

that less than 10–20% was present in the spent media when compared to the total rAAV yield in cell harvests (data not shown). This observation suggests that at the chosen harvest time, optimized for cell harvest, most of the virus is still intracellular or membrane-bound and that our gentle harvest process maintains cellular membrane integrity. Historical data generated by our Vector Core also consistently revealed that less than 10% of free AAV9-GFP is present in spent media upon transfection. This data is in sharp contrast with findings published by other laboratories, as discussed later.

Overall, our results suggested a modest yet consistent increase in vector genome yield per CS10 by HSV-based production. Because of the observation that pellet weights were smaller at the time of harvest upon infection, it suggested that the cell number could be significantly increased for HSV-based protocol. This was also supported by pilot experiments in smaller T225 flasks as well as earlier publications indicating that cell number > 1×10^9 cells or supra confluence could be used in the adherent cell format.[31,32]

Optimized infection protocol results in increased surface and volumetric yields

In view of increasing our overall rAAV9 yield, we attempted to infect approximately two to three times more HEK 293 per CS10. Two additional production runs were performed using 1.5×10^9 cells at the time of infection. Accordingly, based on pellet weight the cell mass

was increased by about 2.15-fold at the time of harvest, confirming that more cells had been infected and harvested. Optimizing cell mass starting material had a dramatic impact on the overall system capability, with a significant, 7.5-fold increase in vector genome yield as compared to transfection and 4.6-fold as compared to previous infection conditions at lower cell number, with an average of 1.59×10^{14} vg of purified AAV9 recovered per CS10 (8.60×10^{13} and 2.3×10^{14} vg from two independent experiments; $P < 0.05$) (Figure 3a and Table 1). This was confirmed with a sixfold increase in the overall yield normalized to cell mass (Table 1).

Increased infectious titers in HSV-generated rAAV9 stocks

A critical criterion for any rAAV manufacturing system and associated processes is the quality of the vector generated in terms of infectivity or potency. Overall, rAAV9 yields were next assessed for all purified stocks based on the infectious unit titer. Infectious titers were measured by two well-accepted methods using an *in vitro* assay based on Ad5-superinfected C12 cells. Transducing titers were calculated based on the number of GFP-expressing cells related to the vector dilution performed; infectious titers were calculated based on the number of replication centers detected by ^{32}P hybridization. Interestingly, we observed a significant net increase in the overall infectious particle yield in HSV infection-generated material with ~6.44 TU/cell, a nearly eightfold increase when compared to transfection. The increased cell number, together with the increased VG/cell and TU/cell resulted in an overall 18-fold increase of total transducing units per CS10 when compared to transfection yields ($P < 0.05$; Figure 3b and Table 1). It is worth noting that the increase in infectious unit titers was greater in all cases than the increase noted for the physical particles (vector genome), suggesting an improved overall potency of the rAAV9 preparations generated by HSV. This resulted in improved ratio of vector genomes to transducing units, which were decreased by 1.5–2.4 times in HSV-produced virus (Table 1).

To further delineate the basis of the observed increase in infectivity, we performed additional *in vitro* characterization. We hypothesized that if a higher percentage of virions produced were infectious, then a higher number of cells should be transduced at a given vector genome amount. To test this hypothesis, Ad5-superinfected C12 cells were infected with increasing titers of equal vector genomes amount (2×10^5 to 1×10^6 vector genomes/cell) of transfection or HSV-made rAAV9-GFP and GFP-positive cells were counted by flow cytometry. There was an approximately 30% increase in GFP-positive cells in HSV-produced vector when compared to transfection (Figure 4). This suggested that indeed a higher percentage of infectious particles were in the HSV-made rAAV9 stocks. We next performed a series of control experiments. First we tested whether the HSV-generated vector matrix would contain any residual cellular/and or viral material that could promote rAAV9 transducing ability *in vitro*. For that purpose, we generated three different control matrices: (i) transfection control matrices consisted of a mock transfection with all the precipitation components and no plasmids, or (ii) the helper plasmid only (rAAV9 empty capsids), (iii) an infection control matrix consisted of an infection with rHSV-GFP only so that no rAAV could be packaged. All controls were produced and purified using the same processes as described above to produce rAAV9-GFP. We next used these matrices as spike-in to Ad5-superinfected C12 cells at various dilutions. C12 cells were also infected with a known amount of rAAV9-GFP stock produced by transfection (approximate MOI of 3×10^2 vg/cell). The results showed that the number of GFP-expressing cells, or transducing

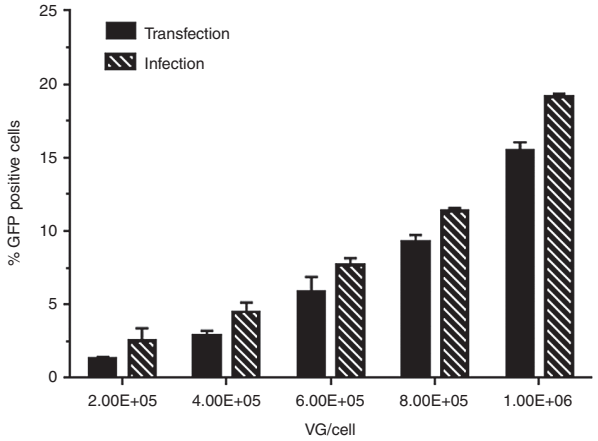

Figure 4 Transduction efficiency. Flow cytometry analysis of C12 cells infected with equal vector genome amounts of transfection or infection made recombinant adeno-associated virus (rAAV)9-GFP. Purified vectors preparations obtained by transfection ($n = 4$) or infection ($n = 5$) were pooled and used to infected cells at various multiplicity of infections and GFP expression detected by FACS10. Average from duplicates with standard deviation are depicted.

units, were identical in all conditions, independently of the vector spike-in. These results demonstrated that there was no cellular and/or HSV viral contaminants in the preparations that could promote rAAV transduction efficiency. It did not preclude, however, the possibility that contaminants may be rAAV9 capsid-bound and copurified with rAAV9-GFP.

Total capsid amount is reduced in HSV-generated stocks

We next assessed the amount of rAAV capsid protein in each of these preparations. An identical number of vector genome particles of each sample were analyzed by soidum dodecyl sulfate polyacrylamide gel electrophoresis (SDS-PAGE) and the total capsid amount per lane was determined semiquantitatively by western blot analysis and coomassie staining. Transfection and infection samples were pooled and a representative image is showed for each experiment (Figure 5a,b). As observed by visual examination of the signals, both coomassie staining and western blot quantification showed a decreased in the overall capsid amount in infection-generated stocks. By densitometry quantification, the coomassie staining of wells containing 10^{10} vector genomes of each sample showed an approximately 32% decrease in the total capsid amount (quantification of VP1+VP2+VP3 proteins), while the western quantification revealed an about 20% reduction.

Next semiquantitative and qualitative data was obtained by electron-microscopy for two representative preparations of rAAV9-GFP for each production method. Count of empty and full capsids revealed 16% full capsids for transfection-generated (Figure 5c) and 28% full capsids for infection-generated (Figure 5d). Overall, these results suggested that a reduced amount of empty capsids was generated by the HSV coinfection method.

Yield and potency are not affected during purification from either method

Last we verified that the overall yield increases observed for HSV-mediated AAV production were independent of the purification processes. We assessed the recovery at each purification step by determining total TU in intermediate samples and did not notice a significant difference between HSV- and plasmid-generated AAV9. Overall,

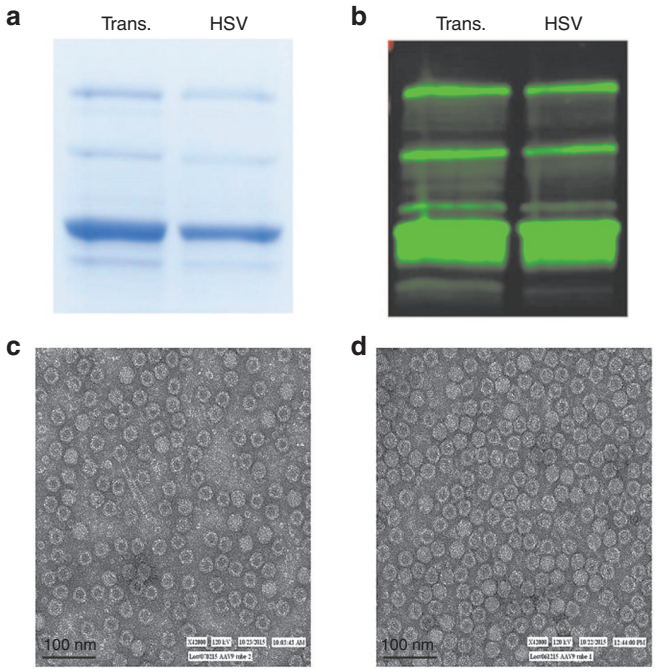

Figure 5 Amount of adeno-associated virus (AAV) capsids from stocks obtained by transfection and infection. (**a**) Coomassie. Stocks obtained by transfection (n = 4) or infection (n = 5) were pooled at equimolar amount and same amount of vector genomes (9.6×10^{10} vg) were loaded on SDS/PAGE prior to staining with Coomassie and quantified. (**b**) Western blotting. Stocks obtained by transfection (n = 4) or infection (n = 5) were pooled at equimolar amount and same amount of vector genomes (1.5×10^{11} vg) were loaded on SDS/PAGE prior to western blotting and imaging. **c**/**d** representative image of electron microscopy by negative staining from **c**: transfection and **d**: Opt. infection.

the purification process had a 50–60% recovery for the chromatography purification step, and > 80% for the tangential flow filtration concentration step, for an overall recovery of approximately 40–50% from the SP load. The recovery from the crude lysates was not determined.

AAV9 stocks purity

Traditionally, we have determined AAV stock chemical purity by coomassie staining and quantification of the overall percentage of AAV9 capsid protein as compared to the other contaminants detected. Purity was determined for each single AAV9 stock and was found to exceed 90% in all preparations without significant difference between the production methods (Table 1 and Figure 5a). We also assessed viral clearance during the purification process. More specifically we determined the rHSV titers at each step of the purification process by plaque assay on V27 cells. Results showed that traces of rHSV were detected in the Benzonase-treated crude lysate step (prior to flocculation). This corresponded to less than 2% (n = 2) of the initial HSV load used in the inoculum. Levels of rHSV were below detection limit (100 PFU/ml) for all the subsequent steps, including SP load, purified bulk (SP peak), and final stock (n = 5) (Table 1). Based on the amount of rHSV in the inoculum, a 100% rHSV clearance was achieved. These results demonstrated that our purification processes were extremely efficient at removing and/or inactivating rHSV particles.

In vivo administration of HSV-produced rAAV9 is safe and efficient

To validate safety and expression from HSV infection made vectors, 129SVE mice received a single intramuscular injection with 1×10^{10} vg per mg of tibialis anterior (TA) muscle. One month postinfection,

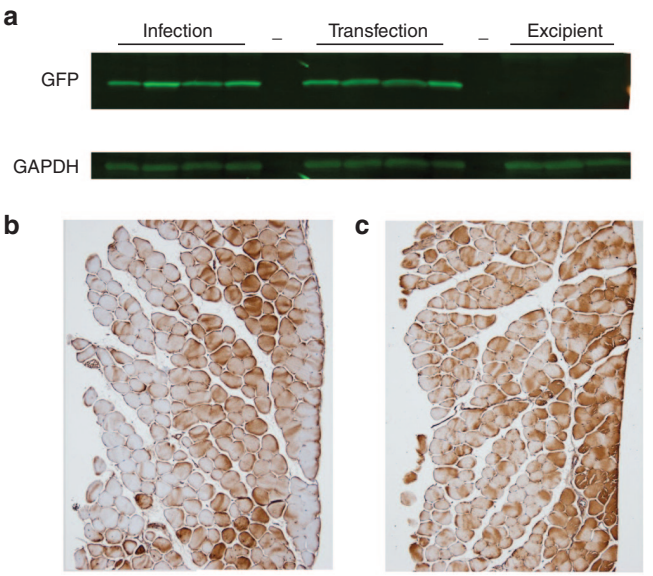

Figure 6 GFP expression in TA muscles of mice injected with infection or transfection made adeno-associated virus (AAV). (**a**) Similar GFP expression was detected in both groups of mice injected with infection or transfection made rAAV9. No expression was observed in excipient only injected groups. (**b**,**c**) Representative sections showing GFP expression by immunohistochemical staining in TA muscles injected with infection (**b**) or transfection (**c**) made rAAV9.

GFP expression was determined by western blot and immunohistochemical analysis, and adverse reactions were evaluated by H&E staining of muscle tissues. Overall GFP expression, as detected by western blot densitometry quantification, was similar in both animal groups injected with infection or transfection made rAAV9 (5.91 ± 1.6 versus 5.75 ± 1.1 arbitrary units, respectively) (Figure 6a). Immuno-histochemical analysis showed similar distribution of transgene expression in muscle fibers in both groups (Figure 6b,c), and no increase in inflammatory cells or tissue damage was observed by H&E staining in any of the injected groups (data not shown). These data indicate that infection made rAAV9 performs equivalent to transfection made vector *in vivo* and is safely tolerated at relatively high doses in intramuscular injections.

DISCUSSION

To our knowledge, this is the first study providing an in-depth and side-by-side comparison of the HSV manufacturing system versus the transfection method for the production of AAV serotype 9. In this study, we report a four to fivefold increase of AAV yield per unit of production when using the HSV coinfection protocol directly compared to the transfection method, with vector genomes in excess of 1×10^{14} vg per CS10 or approximately 1×10^{5} vg per cells. This overall yield increase was the result of a combination of at least two parameters compared to transfection, as documented in this study: (i) ~2.5-fold higher cell number at the time of infection per unit of production (T225 or CS10 and (ii) a greater than twofold increase of vg per cell. This is also the first detailed study describing a complete protocol for the manufacturing and purification of HSV-made AAV serotype 9 suitable for preclinical GLP studies, that could be readily implemented in the GMP setting for clinical or commercial AAV manufacturing. In contrast to many other studies on AAV manufacturing, the yields reported in this work, both for transfection and infection, are from preparations that underwent a complete purification process using a protocol currently used in

our Human Applications Laboratory for the manufacture of clinical grade AAV9.[37]

Production of rAAV using the HSV system has previously been reported by several groups including ours[29,30,32,39,40] (also reviewed in ref. 41), with an emphasis on AAV serotypes 1 and 2 (refs. 31,32) and with very limited or incomplete data provided for serotype 9.[31] For instance, in a study published by Kang and colleagues, the total VG yield or the VG:cell of fully purified AAV1 or AAV9 stocks were not disclosed,[31] rendering direct comparison to our study difficult. In this study, however, the vg titer was reduced by about twofold for AAV1 when produced by infection in HEK293 as compared to transfection. This is in sharp contrast with our results for AAV9 that demonstrated a net increase in both vector titers and total vector genome yield for infection-made stocks.

Perhaps, the most critical observation from our work was that the HSV system was capable of generating fully infectious and stable AAV9 particles. We report a near 18-fold increase in total infectious units from HSV-based material when compared to transfection-produced material per CS10. The increased infectivity was reflected by a reduction of the vector genome-to-infectious particle ratio in excess of 2.5-fold. This is an unprecedented observation for AAV serotype 9. In the above discussed study by Kang *et al.*, production of a biologically active rAAV9 stock using the HSV method was demonstrated upon intra-muscular administration to mice and direct measurement of the transgene expression in serum.[31] In the same study, the authors also obtained a significantly lower vector genome-to-infectious particle ratio in HSV-produced rAAV1 when compared to transfection-produced AAV1, which was then correlated to a superior transgene expression in animals injected intramuscularly.[31] These results convincingly showed a superior transducing capability of AAV1 stocks made by the HSV system when compared to transfection. However, this study did not determine whether the higher expression was a result of increased cell transduction or improved transgene expression per cells, and the comparison with transfection was not documented for AAV9. But taken together with our results, one could hypothesize that the increased potency of HSV-derived AAV particles may be an intrinsic benefit of this method. Whether this can be truly extended to other AAV serotypes remain to be demonstrated.

Other AAV features pertaining to capsid amount, quality, and overall potency were also analyzed. We showed a reduction of the overall capsid amount in infection-produced stocks, correlated with a lower amount of empty capsids. These findings are in line with similar findings previously reported for AAV1.[31,42] However, it is not known whether the reduced amount of empty capsids is the basis for the overall increased infectivity. Interestingly, we also showed that once all our AAV9 stocks were standardized to identical transducing/infectious unit titers, the overall number of infected cells was about twofold higher for HSV-made products *in vitro*. This suggested that the superior infectivity may be linked to a capsid property that would promote cell infection and/or the AAV genome delivery to the nucleus. The molecular mechanism to explain AAV9 increased vector yields and infectivity is likely a combination of factors in which the natural helper functions of HSV are able to promote stable capsid assembly and encapsidation of the AAV genome. Experiments to further study the capsid structure, the ratio between full and empty capsids as well as the expression ratio of AAV9 VP1, 2, and 3 in the capsid, are currently in progress.

AAV9 stocks generated for this study have been assayed over several months using a series of freeze-thaws and no difference was observed between the transfection and the infection-generated material, suggesting similar capsid stability under usual laboratory conditions. Further, the low pH-excipient used to formulate and store our GLP and GMP AAV9 preparations supported high AAV9 stability probably by limiting the capsid endogenous protease activity as reported in earlier work.[37]

Our work demonstrated successful rAAV9 production when using the HEK 293 adherent system with the HSV coinfection method. However, an obvious challenge of using HEK 293 in an adherent production format is its inherent limitation for large-scale manufacturing and scale-up. Thomas *et al.*[32] developed an AAV production platform using HSV coinfection in suspension-adapted BHK21 cells in disposable bioreactors to support preclinical and clinical scales of rAAV1.[36,42] Favorable features such as lower VG:IU and empty–to-full capsid ratios were maintained,[42] as observed earlier in HEK 293. The authors also reported successful production of serotypes 2, 5, and 8 at a smaller research scale. However, the overall yield appeared significantly lower than the ones obtained for AAV9 in our current work. The authors reported an overall yield of 1×10^{16} vg from a 100L BHK total crude lysate. With a final recovery of about 23%, we calculated that approximately 2.3×10^{15} vg of final product, or 2.3×10^{13} vg per liter of infected BHK cells were produced, resulting in approximately 1.4×10^{4} vg/cell (~1.5×10^{11} cells from a 100L batch). In our study, we report volumetric yields for AAV9 (1 CS10 = 1L volumetric unit) of about twofold and fivefold higher in our current adherent HEK 293 transfection and infection protocols, respectively. Our final yield per cell was also significantly higher, both from transfection and infection methods, with a net increase of about sevenfold for the infection-based method. The most obvious reason for this difference likely relates to the difference in the serotype produced as well as the purification methods used. Other variables including variability in vector genome quantification across laboratories or between different clones of HEK 293 cells also render direct yield comparison difficult.

Yields of purified vector in the range published in this study have not been reported from other methods, for any AAV serotype or construct. Yields as high as 3×10^{13} vg per liter of purified material were recently obtained for rAAV9 using a transfection method in a suspension format of HEK 293 cells, about three times lower than the yields reported in this work.[21] In the same study, ratios VG:TU or VG:IU as low as $1–2\times10^{3}$ were reported for AAV9 as well as an earlier work by Vandenberghe *et al.*[43] This would suggest a higher infectivity than the ones reported in this current work. However, in the same study, Grieger *et al.* reported a ratio for AAV1 stocks around 1×10^{2} and 1×10^{3} for AAV2, a serotype that typically outperforms the other serotypes in HeLa-cells based assays. These results are in sharp contrast with historical data acquired by our core over more than a decade for these three serotypes. Despite an apparent similarity to the assays used by all groups, the cell lines, the detection and calculation may greatly differ (GFP, FACS, Q-PCR, TCID50 or ^{32}P). Therefore, direct comparison from group to group of AAV preparations titers, whether for vector genome or infectious units, must be reported carefully.

When using the baculovirus system, another production method utilizing a suspension cell format, Mietzche and colleagues reported yields ranging from 1×10^{5} vg/cell or up to 2×10^{14} vg per liter of cell culture in cell crude lysates.[27] Unfortunately, the AAV yields postpurification were not disclosed in this study. Note worthily, the same study showed a two- to threefold decrease in the infectious titers for AAV9,[27] using a similar titration method than ours, which is in sharp contrast with our results. However, these data were in line with previous studies revealing the somewhat challenges to produce

infectious particles for serotypes other than AAV2, when using the BAC system.[25,34,35,44] Lower infectious titers could in some cases be overcome by elaborated genetic modifications[25,35] or compensated by inflated cell density and higher volumetric scale.[26,27]

In our production protocols, both from $CaPO_4$ transfection or HSV coinfection, the majority of AAV9 infectious particles are present in the cell harvests, with a relatively inconsequential amount in the spent media. This is in sharp contrast with other studies reporting AAV9 particles in excess of 60–80% in the medium after transfection.[21,43,45] While the definitive basis of this difference is not known at this time, it is likely due to differences within the transfection protocol ($CaPO_4$/PEI), the HEK293 clone used, the time of harvest (2–3 versus 5 days), harvest procedure (gentle PBS wash or PBS/EDTA cell detachment versus the use of NaCl). Similarly, we did not observe a significant amount of rAAV9 in the spent medium after HSV infection. The most obvious reason for this finding may lie on an early harvest time point (48 hours).

The many advantages to the HSV-based production system are most evident for large scale of 1×10^{15} vg or more for use in preclinical and clinical studies. Creating the different recombinant HSVs, the viral banks and pilot runs would take an average of 4 to 6 months of upstream work prior to starting the AAV production campaign. Transfection will remain the most versatile and affordable method for small-scale, short turn-around studies for quick evaluation of various AAV constructs. For large-scale however, the time invested up front would largely be recovered by the ability to generate high-titer AAV stocks at high potency with the HSV system.

The HSV method, like all the methods developed to date, may present some challenges when entering the commercialization platform and requirements. The purity of the rAAV9 preparations will need to be thoroughly assessed. However, earlier preclinical and clinical studies clearly demonstrated the safety of HSV-made AAV1 preparations.[36,42] The versatility of the system to other AAV constructs and serotypes is supported by previously published work as well as ongoing studies in our laboratory. While the overall titers obtained for different AAV constructs may greatly vary, the four- to fivefold increase observed in the current work when compared to transfection material seems to remain consistent (to be published).

Together, our work is the first to date to describe a complete production and purification method for AAV9. This method leads to a significant improvement in both rAAV9 yields and vector quality. It is, to our knowledge, the only production method published that enabled generation of high titer of highly infectious particles without the need of complex genetic regulation mechanisms. The method is currently used in our Core to generate GLP-grade stocks for preclinical studies and is readily translatable to large-scale GMP production of rAAV9 vectors for early phase studies and commercialization of AAV manufacturing.

MATERIALS AND METHODS

Cells, plasmids, and viruses

Cell lines. HEK 293 were maintained in Dulbecco's modified Eagle medium (DMEM) (Hyclone, GE Healthcare, Logan, UT) supplemented with 5% fetal bovine serum (FBS) (Corning, Corning, NY) and 1% antibiotic/antimycotic (Gibco, ThermoFisher Scientific, Waltham, MA). V27 (a gift from Dr. Knipe,[46]) and C12 (a gift from Dr. P. Johnson,[47] cells were maintained in DMEM supplemented with 5% FBS, and 50 µg/ml Geneticin (Sigma, St. Louis, MO).

AAV plasmids. Plasmid pTR-UF5 was been previously described.[23,48–50] AAV9 Helper plasmid, pDG-UF9-KanR was created by ligating the AAV2 Rep and AAV9 Cap sequences from plasmid pMA-P5-Rep2/Cap9 into pDG-KanR using Sal I and Cla I. Plasmid pDG-KanR is a derivative of pDG[22] in which AmpR was replaced by KanR. Plasmid pMA-P5-Rep2/Cap9 was created by inserting the synthesized cassette containing AAV2 Rep from the Nco I site, AAV9 Cap, and AAV2 poly-adenylation sequences (GeneArt, ThermoFisher) in plasmid pMA-P5-Rep2 containing the AAV2 P5 and AAV2 Rep (up to the Nco I site) sequences (GeneArt, ThermoFisher). For transfection, research-grade plasmid preparations were obtained from Aldevron (Fargo, ND).

Plasmid pHSV106-MCS was constructed by inserting a linker sequence (multiple cloning sites) within the unique Xba I site of pHSV106-Xba.[29] Plasmid pHSV106-AAV2/9 was generated by inserting the P5-AAV2 Rep—AAV9 Cap sequences into pHSV106-MCS. The P5-Rep2Cap9 cassette was obtained by first synthesizing the AAV2 P5 promoter region upstream of the AAV2 Rep sequence (GeneArt, ThermoFisher) up to the Nco I site to obtain plasmid pMA-P5-Rep2. In this cassette, the AAV2 Rep ATG was replaced by an ACG to mimic Conway's construct.[51] Next, the remaining AAV2 Rep and the complete AAV9 Cap sequences was inserted into pMA-P5-Rep2. The AAV9 cassette was obtained either from plasmid pAAV2/9, obtained from Dr. J. Wilson, University of Pennsylvania, or from a synthesized sequence (GeneArt, ThermoFisher). Plasmid pHSV106-UF5 was previously described and contains the AAV-CMV-GFP genome cassette from plasmid pTRUF5.[29]

Recombinant viruses. Recombinant herpes viruses were generated by homologous recombination as previously reported.[30] Briefly, V27 cells were transfected in six-well plate with a linearized plasmid pHSV106-AAV2/9 using Fugene HD (Promega, Madison, WI) in the presence of rHSV-GFP HSV DNA obtained from infected V27 with a source stock of virus rHSV-GFP. After 3–4 days, cells were harvested by freeze-thaws and serial dilutions of the lysates were used to infect V27 cells for 1 hour, followed by 0.8% soft-agar overlay (LMT Agar, Life Technologies, ThermoFisher). Plaques selection was performed approximately 3–4 days postinfection under microscopy for selection of clear, non GFP-expressing cell-formed plaques. Each individual plaque was then further selected by two rounds of plaque selection to ensure removal of rHSV-GFP infected cells. Individual plaques were tested for the presence of the AAV2/9 cassette by Q-PCR and plaque assay of infected cell lysates. The best clonal plaques were selected for further amplification for the preparation of Master Seed Stocks. RHSV-UF5/GFP had already been generated from previous work.[29]

Production of rHSV seed stocks. Seed stocks were prepared on V27 at ~80–90% confluency (~$5–8\times10^8$ cells per CS10 (Corning). HSV was added to the medium at an approximate MOI of 0.1 to 0.3 pfu/cell. Three days postinfection, cells were lysed *in situ* at 0.6M NaCl (5M NaCl, Accugene) and harvested. After approximately 30 minutes, the lysates were collected and cell debris removed by centrifugation (3,000 revolutions per minute (RPM), 20 minutes, 4 °C). HSV-containing lysate was concentrated approximately 10-fold by Tangential Flow Filtration using TangenX Sius-300 kDda (Cat# XP300L01L, TangenX, Shrewsbury, MA). After addition of Glycerol (5% final concentration, ThermoFisher), stocks were aliquoted and stored frozen at negative −80 °C.

HSV assays

Plaque assay. HSV seed stocks infectious titers were assessed by a traditional plaque assay. V27 cells were seeded at 1.2×10^5 cells per well in 24-well plates (Corning). Serial dilutions of the HSV stocks were added to the cells and incubated for 1.5–2 hours. The inoculate was removed and DMEM containing 0.8% agar (LMT Invitrogen) was poured in each well. Plaques were counted under microscope 72 hours postinfection. Plaque staining was utilized to detect replication-competent HSV in purified AAV preparations and was performed similar to previously described method.[31]

AAV9 production and purification

AAV9 was produced by transfection or co-infection with HSV on HEK 293 plated in Corning T225 Flasks (Corning) or CS1010 (Corning, 10-STACKS, 6,360 cm^2 cell growth area).

Transfection. Standard $CaPO_4$-mediated transfection of plasmids was performed as previously described.[23] Briefly, plasmid pTRUF5 and pDG-UF9-KanR were transfected at 1:1 molar ratio (18 and 65 µg, respectively in T225, and 0.62 and 1.87 mg respectively in CS10) in 70% confluent 293 and incubated for 72 hours. On day of harvest, cells were detached using 1× Dulbecco's phosphate buffer saline (DPBS)/5 mmol/l EDTA, rinsed with 1× DPBS and pelleted at 1,500 RPM, 4 °C for 15 minutes. Pellet weights were recorded and stored frozen at negative 80 °C.

Infection. HEK 293 was infected when confluency reached between 80 and 100%. Cells were counted on day of infection and the calculated amount of each rHSV stocks was added to fresh DMEM for the desired MOIs. Cells

were dislodged from the flask by gentle shaking 48–52 hours postinfection followed by centrifugation (2,000 RPM, 20 minutes, 4 °C) and one PBS wash. Pellet weights were recorded and stored frozen at negative 80 °C. For T225, cell pellets were resuspended in 5 ml of lysis buffer (150 mmol/l Tris, 50 mmol/l NaCl, pH 8.5) and submitted to three cycles of freeze-thaws.

AAV9 purification. The pellet was thawed at 37 °C and processed for virus purification as previously described.[37] Briefly, the cell pellet was first resupsended in water for injection and a sodium citrate buffer (30.63 mmol/l final concentration) containing 1 mmol/l $MgCl_2$ and 30 U/ml Benzonase (EMD Chemicals, Billerica, MA). The reaction was incubated for 1 hour at 37 °C with regular swirling. Flocculation was performed by adding citric acid and water for injection to a final concentration of approximately 30.6 mmol/l. The protein flocculate was clarified by centrifugation (4,000 RPM, 10 minutes, 22 °C) and the virus-containing supernatant (SP load) was loaded onto a sanitized HiPrep SP FF (20 ml bed volume, GE Healthcare Life Sciences, Pittsburg, PA) and pre-equilibrated with buffer A (8 mmol/l sodium citrate, 16 mmol/l citric acid) and buffer B (42.8 mmol/l sodium citrate, 7.2 mmol/l citric acid, 0.5M sodium chloride). Virus was eluted as a discreet peak (SP Peak, 40% buffer B) in a final formulation of 22 mmol/l sodium citrate, 13.1 mmol/l citric acid and 200 mmol/l sodium chloride, at ~pH 4.8 The sample was then sterile filtered with Millex-GV syringe filter, 0.22 µmol/l (EMD Millipore) and stored frozen at −80 °C (Purified Bulk). The virus was further concentrated by tangential flow filtration using a 100K NMWC Midgee Hollow Fiber cartridge (GE Healthcare Life Sciences) and filter sterilized (Final stock).

AAV testing

Vector genome titer. Vector genome titers were obtained by quantitative real-time PCR (Q-PCR). Vector stocks were submitted to RNase-free DNase I digestion (New England BioLabs, Ipswich, MA) (20 U/ml, 30 minutes, 37 °C) and diluted six times in RNAse-DNAse-free water (Gibco) using a fivefold dilution scheme (5×10^2-fold to 1.56×10^6-fold). PCR reactions were prepared according to manufacturer's instructions: 1× iQ SYBR Green Supermix (Bio-Rad, Hercules, CA), 200 nmol/l UF5-3F and UF5-3R primers, 95 °C 10 minutes, 95 °C 10 seconds, 62 °C 30 seconds, 40 cycles (CFX Connect Real-Time System, Bio-Rad). A standard curve was prepared using pTRUF5 plasmid loaded at 1.32×10^2 to 1.32×10^7 copy numbers per reaction over a 10-fold dilution scheme). All dilutions were averaged for each sample for a coefficient of variability (CV) less than 25%. PCR was repeated three independent times and values averaged for each stock.

Droplet digital PCR. DNase-digested vector stocks were submitted to droplet generation and genomic amplification using 1× QX200 ddPCR EvaGreen Supermix, and each 100 nmol/l of UF5-3F and UF5-3R primers (Bio-Rad). Droplet generation and reading was performed by the Interdisciplinary Center for Biotechnology Research, UF, with the same cycling conditions as above using Bio-Rad's QX200 Droplet Digital System. Two independent ddPCR runs were used to calculate the average value for each stock.

Dot blot. Dot blot were performed as previously described using pTRUF5 as standard curve and CMV specific ^{32}P-radiolabeled probe.[37] Titers represent the average values from two to three independent assays.

Infectious center assay. Ad5-infected C12 were infected in 96-wells by serial dilutions of the AAV-containing samples. After ~42 hours, infected cells were transferred to a nylon membrane (GE Healthcare) using a vacuum device. Viral DNA was denatured and fixed to the membrane by one cycle of denaturation (Denaturing solution, Sigma) and one cycle of neutralization (Neutralizing solution, Lonza, Allendale, NJ) followed by UV Crosslinking. Viral DNA was detected by in situ ^{32}P hybridization using a CMV specific ^{32}P-labeled DNA fragment and exposure to radio films (Kodak, Rochester, NY). Titers were calculated based on the number of dots obtained at corresponding dilutions, from two to three independent assays.

Transduction assay. Ad5-infected C12 cells were infected in 96-well plates by serial dilutions of the AAV-containing samples. After 42–48 hours, GFP-expressing cells were visually counted under microscopy and titer calculated and average from three independent assays.

Identity and purity assay. Purity and capsid amount were assessed by Coomassie staining. Stocks were diluted at the same vg/ml in AAV9 excipient (elution buffer) and 9.6×10^{10} vg were separated on a 10% SDS-polyacrylamide gel (Bio-Rad). Gel was staining using GelCode Blue (Pierce, ThermoFisher) and scanned. Purity was assessed by quantification of VP1/2/3 and derivatives and is expressed as a percentage of total protein detected and quantified by the imaging software Quantity One (Bio-Rad). For image purposes, the same stocks were pooled at equimolar amount and the pool was run for imaging.

Western blotting. Purified vector preparations were prepared like for the Coomassie staining except that 1×10^{10} vg vector genomes were separated on a 10% SDS-polyacrylamide gel (Bio-Rad) and transferred to nitrocellulose membrane. AAV capsid proteins were detected using an anti-AAV capsid antibody (ARP American Research Product, Waltham, MA) at a dilution of 1:2,000 and a goat anti-mouse infrared conjugated secondary at 1:10,000. Blots were visualized and quantified using an infrared imaging system and accompanying software (LiCor, Lincoln, NE).

Electron-microscopy. Negative staining EM was performed by the laboratory of Dr. Mavis Agbanje-McKenna, Department of Biochemistry and Molecular Biology, Center for structural Biology, UF using standard technique. Briefly preparations used to determine EM were concentrated using Apollo 150 kDa to reach titers > 1×10^{13} vg/ml. Samples were adhered to glow-discharged carbon-coated copper grids (TED Pella, Redding, CA) and stained with 2% uranyl acetate. Full and empties were manually counted using the same scale picture field for each stock. Three independent pictures were used for the count, and results averaged.

Flow cytometry. Ad5-infected C12 cells were infected with 2×10^5 to 1×10^6 vector genomes per cell of each lot of transfection or HSV made AAV expressing GFP or a pooled sample containing equal amount of each stock at a final concentration of 3×10^{12} vector genomes per ml. At 48 hours postinfection, cells were washed in PBS and suspended in 1% paraformaldehyde. Cell sorting for eGFP expression was performed on a FACS10 Calibur (BD Biosciences, San Jose, CA) and analyzed using CellQuest Version 3.3. Each experiment was run with 10,000 cells, and untreated, Ad5-only, and AAV-transduced cells were compared. Each experiment was performed in triplicate and results are reported as total percentage of GFP-positive cells.

In vivo testing

Experimental animals. Two-month-old male 129SVE mice were randomized to the following groups: untreated + excipient, AAV9-GFP (infection made) + excipient, or AAV9-GFP (transfection made) + excipient. All animal studies were approved in accordance with the guidelines set forth by the University of Florida Institutional Animal Care and Use Committee. All animals were sacrificed at 3 months of age (1 month postinjection) for molecular and histologic assays.

In vivo delivery of rAAV vector. Mice were anesthetized using 2% isoflurane (1l O2). Under sterile conditions, mice were injected with a single injection using an insulin tuberculin syringe. Excipient solution (vehicle made of 22 mmol/l sodium citrate, 13.1 mmol/l citric acid, and 200 mmol/l sodium chloride, at ~pH 4.8) or rAAV9 (1×10^{10} vg/mg of tibialis anterior muscle) diluted with excipient solution to a quantity sufficient volume of 20 µl was used for intramuscular delivery.

Western blotting. Protein was extracted from tibialis anterior muscles were with RIPA buffer containing protease inhibitor cocktail (Roche Applied Science, Indianapolis, IN). Twenty micrograms of protein lysates were separated by gel electrophoresis and transferred to a nitrocellulose membrane. GFP proteins were detected using a chicken anti-GFP antibody (Aves Labs, Tigard, OR) at a dilution of 1:2,000 and an anti-chicken infrared conjugated secondary at 1:10,000. Blots were visualized and quantified using an infrared imaging system and accompanying software (LiCor, Lincoln, NE). The bands were quantified by densitometry and normalized to glyceraldehyde 3 phosphate dehydrogenase (GAPDH) loading control.

Hematoxylin and eosin (H&E) staining. Sections were stained with hematoxylin and eosin for the presence of inflammation or myofiber damage in transverse sections of the tibialis anterior muscle and imaged using bright-field microscopy.

Immunohistochemistry. GFP immunohistochemistry of the tibialis anterior muscle was performed as previously described.[15,52] Briefly, transverse tissue sections were incubated overnight with primary antibody against GFP, diluted 1:1,000 (chicken anti-GFP; Aves Laboratories, Tigard, OR). Sections were washed in phosphate-buffered saline, incubated with a biotinylated

anti-chicken IgG secondary antibody (diluted 1:200; Vector Laboratories, Burlingame, CA), and treated with a VECTASTAIN ABC kit and DAB for detection via bright-field microscopy.

Statistical analysis. All bar graph results are presented as mean ± standard deviation. A grouped unpaired Student's *t*-test was used to compare differences between vector genomes, transducing units, pellet weight, and fast protein liquid chromatography area under the curve. *P* values < 0.05 were considered statistically significant.

CONFLICT OF INTEREST

L.A.S., M.P., B.D.C., and N.C. declare no conflict of interest. B.J.B. is an inventor of intellectual property owned by the Johns Hopkins University and the University of Florida related to this research and could be entitled to patent royalties for inventions described in this manuscript.

ACKNOWLEDGMENTS

This work was partly supported by the US Department of Defense W81XWH-13-1-0283 to B.J.B. The authors would like to thank Bloom, University of Florida, for constructive discussion related to HSV, Paul Chipman, and Mavis Agbanje-McKenna for performing EM and helpful discussion on AAV9 capsid, and the staff of the Powell Gene Therapy Center Vector Core for technical assistance.

REFERENCES

1. Clement, N and Grieger, J (2016). Manufacturing of recombinant adeno-associated vectors for clinical trials. *Mol Ther Methods*, **3**: 16002.
2. Todd, AG, McElroy, JA, Grange, RW, Fuller, DD, Walter, GA, Byrne, BJ *et al.* (2015). Correcting neuromuscular deficits with gene therapy in Pompe disease. *Ann Neurol* **78**: 222–234.
3. Mendell, JR, Rodino-Klapac, L, Sahenk, Z, Malik, V, Kaspar, BK, Walker, CM *et al.* (2012). Gene therapy for muscular dystrophy: lessons learned and path forward. *Neurosci Lett* **527**: 90–99.
4. Mah, CS, Soustek, MS, Todd, AG, McCall, A, Smith, BK, Corti, M *et al.* (2013). Adeno-associated virus-mediated gene therapy for metabolic myopathy. *Hum Gene Ther* **24**: 928–936.
5. Ramos, J and Chamberlain, JS (2015). Gene Therapy for Duchenne muscular dystrophy. *Expert Opin Orphan Drugs* **3**: 1255–1266.
6. Smith, BK, Collins, SW, Conlon, TJ, Mah, CS, Lawson, LA, Martin, AD *et al.* (2013). Phase I/II trial of adeno-associated virus-mediated alpha-glucosidase gene therapy to the diaphragm for chronic respiratory failure in Pompe disease: initial safety and ventilatory outcomes. *Hum Gene Ther* **24**: 630–640.
7. Byrne, BJ, Smith, B, Mah, C, Lawson, LA, Islam, S, Corti, M, *et al.* (2014). Phase I/II trial of diaphragm delivery of recombinant adeno-associated virus acid alpha-glucosidase (rAAV1-CMV-GAA) gene vector in patients with Pompe disease. *Hum Gene Ther Clin Dev* **25**: 134–163.
8. Kornegay, JN, Spurney, CF, Nghiem, PP, Brinkmeyer-Langford, CL, Hoffman, EP and Nagaraju, K (2014). Pharmacologic management of Duchenne muscular dystrophy: target identification and preclinical trials. *ILAR J* **55**: 119–149.
9. Mulcahy, PJ, Iremonger, K, Karyka, E, Herranz-Martín, S, Shum, KT, Tam, JK *et al.* (2014). Gene therapy: a promising approach to treating spinal muscular atrophy. *Hum Gene Ther* **25**: 575–586.
10. Inagaki, K, Fuess, S, Storm, TA, Gibson, GA, Mctiernan, CF, Kay, MA *et al.* (2006). Robust systemic transduction with AAV9 vectors in mice: efficient global cardiac gene transfer superior to that of AAV8. *Mol Ther* **14**: 45–53.
11. Pacak, CA, Mah, CS, Thattaliyath, BD, Conlon, TJ, Lewis, MA, Cloutier, DE *et al.* (2006). Recombinant adeno-associated virus serotype 9 leads to preferential cardiac transduction in vivo. *Circ Res* **99**: e3–e9.
12. Pacak, CA, Sakai, Y, Thattaliyath, BD, Mah, CS and Byrne, BJ (2008). Tissue specific promoters improve specificity of AAV9 mediated transgene expression following intravascular gene delivery in neonatal mice. *Genet Vaccines Ther* **6**: 13.
13. Bevan, AK, Duque, S, Foust, KD, Morales, PR, Braun, L, Schmelzer, L *et al.* (2011). Systemic gene delivery in large species for targeting spinal cord, brain, and peripheral tissues for pediatric disorders. *Mol Ther* **19**: 1971–1980.
14. DeRuisseau, LR, Fuller, DD, Qiu, K, DeRuisseau, KC, Donnelly, WH Jr, Mah, C *et al.* (2009). Neural deficits contribute to respiratory insufficiency in Pompe disease. *Proc Natl Acad Sci USA* **106**: 9419–9424.
15. ElMallah, MK, Falk, DJ, Lane, MA, Conlon, TJ, Lee, KZ, Shafi, NI *et al.* (2012). Retrograde gene delivery to hypoglossal motoneurons using adeno-associated virus serotype 9. *Hum Gene Ther Methods* **23**: 148–156.
16. Gregorevic, P, Blankinship, MJ, Allen, JM, Crawford, RW, Meuse, L, Miller, DG *et al.* (2004). Systemic delivery of genes to striated muscles using adeno-associated viral vectors. *Nat Med* **10**: 828–834.
17. Kornegay, JN, Li, J, Bogan, JR, Bogan, DJ, Chen, C, Zheng, H *et al.* (2010). Widespread muscle expression of an AAV9 human mini-dystrophin vector after intravenous injection in neonatal dystrophin-deficient dogs. *Mol Ther* **18**: 1501–1508.
18. Falk, DJ, Mah, CS, Soustek, MS, Lee, KZ, Elmallah, MK, Cloutier, DA *et al.* (2013). Intrapleural administration of AAV9 improves neural and cardiorespiratory function in Pompe disease. *Mol Ther* **21**: 1661–1667.
19. Falk, DJ, Soustek, MS, Todd, AG, Mah, CS, Cloutier, DA, Kelley, JS *et al.* (2015). Comparative impact of AAV and enzyme replacement therapy on respiratory and cardiac function in adult Pompe mice. *Mol Ther Methods Clin Dev* **2**: 15007.
20. Blankinship, MJ, Gregorevic, P and Chamberlain, JS (2006). Gene therapy strategies for Duchenne muscular dystrophy utilizing recombinant adeno-associated virus vectors. *Mol Ther* **13**: 241–249.
21. Grieger, JC, Soltys, SM and Samulski, RJ (2016). Production of recombinant adeno-associated virus vectors using suspension HEK293 cells and continuous harvest of vector from the culture media for GMP FIX and FLT1 clinical vector. *Mol Ther* **24**: 287–297.
22. Grimm, D, Kern, A, Rittner, K and Kleinschmidt, JA (1998). Novel tools for production and purification of recombinant adenoassociated virus vectors. *Hum Gene Ther* **9**: 2745–2760.
23. Zolotukhin, S, Potter, M, Zolotukhin, I, Sakai, Y, Loiler, S, Fraites, TJ Jr *et al.* (2002). Production and purification of serotype 1, 2, and 5 recombinant adeno-associated viral vectors. *Methods* **28**: 158–167.
24. Clark, KR (2002). Recent advances in recombinant adeno-associated virus vector production. *Kidney Int* **61**(1 Suppl): S9–15.
25. Aslanidi, G, Lamb, K and Zolotukhin, S (2009). An inducible system for highly efficient production of recombinant adeno-associated virus (rAAV) vectors in insect Sf9 cells. *Proc Natl Acad Sci USA* **106**: 5059–5064.
26. Cecchini, S, Virag, T and Kotin, RM (2011). Reproducible high yields of recombinant adeno-associated virus produced using invertebrate cells in 0.02- to 200-liter cultures. *Hum Gene Ther* **22**: 1021–1030.
27. Mietzsch, M, Grasse, S, Zurawski, C, Weger, S, Bennett, A, Agbandje-McKenna, M *et al.* (2014). OneBac: platform for scalable and high-titer production of adeno-associated virus serotype 1-12 vectors for gene therapy. *Hum Gene Ther* **25**: 212–222.
28. Virag, T, Cecchini, S and Kotin, RM (2009). Producing recombinant adeno-associated virus in foster cells: overcoming production limitations using a baculovirus-insect cell expression strategy. *Hum Gene Ther* **20**: 807–817.
29. Conway, JE, Rhys, CM, Zolotukhin, I, Zolotukhin, S, Muzyczka, N, Hayward, GS *et al.* (1999). High-titer recombinant adeno-associated virus production utilizing a recombinant herpes simplex virus type I vector expressing AAV-2 Rep and Cap. *Gene Ther* **6**: 986–993.
30. Conway, JE, Zolotukhin, S, Muzyczka, N, Hayward, GS and Byrne, BJ (1997). Recombinant adeno-associated virus type 2 replication and packaging is entirely supported by a herpes simplex virus type 1 amplicon expressing Rep and Cap. *J Virol* **71**: 8780–8789.
31. Kang, W, Wang, L, Harrell, H, Liu, J, Thomas, DL, Mayfield, TL *et al.* (2009). An efficient rHSV-based complementation system for the production of multiple rAAV vector serotypes. *Gene Ther* **16**: 229–239.
32. Thomas, DL, Wang, L, Niamke, J, Liu, J, Kang, W, Scotti, MM *et al.* (2009). Scalable recombinant adeno-associated virus production using recombinant herpes simplex virus type 1 coinfection of suspension-adapted mammalian cells. *Hum Gene Ther* **20**: 861–870.
33. Urabe, M, Ding, C and Kotin, RM (2002). Insect cells as a factory to produce adeno-associated virus type 2 vectors. *Hum Gene Ther* **13**: 1935–1943.
34. Kohlbrenner, E, Aslanidi, G, Nash, K, Shklayev, S, Campbell-Thompson, M, Byrne, BJ, *et al.* (2005). Successful production of pseudotyped mosaic rAAV vectors using a modified baculovirus expression system. *Molecular Therapy* **11**: S155–S155.
35. Mietzsch, M, Casteleyn, V, Weger, S, Zolotukhin, S and Heilbronn, R (2015). OneBac 2.0: Sf9 cell lines for production of AAV5 vectors with enhanced infectivity and minimal encapsidation of foreign DNA. *Hum Gene Ther* **26**: 688–697.
36. Flotte, TR, Trapnell, BC, Humphries, M, Carey, B, Calcedo, R, Rouhani, F *et al.* (2011). Phase 2 clinical trial of a recombinant adeno-associated viral vector expressing α1-antitrypsin: interim results. *Hum Gene Ther* **22**: 1239–1247.
37. Potter, M, Lins, B, Mietzsch, M, Heilbronn, R, Van Vliet, K, Chipman, P *et al.* (2014). A simplified purification protocol for recombinant adeno-associated virus vectors. *Mol Ther Methods Clin Dev* **1**: 14034.
38. Knop, DR and Harrell, H (2007). Bioreactor production of recombinant herpes simplex virus vectors. *Biotechnol Prog* **23**: 715–721.
39. Booth, MJ, Mistry, A, Li, X, Thrasher, A and Coffin, RS (2004). Transfection-free and scalable recombinant AAV vector production using HSV/AAV hybrids. *Gene Ther* **11**: 829–837.
40. Toublanc, E, Benraiss, A, Bonnin, D, Blouin, V, Brument, N, Cartier, N *et al.* (2004). Identification of a replication-defective herpes simplex virus for recombinant adeno-associated virus type 2 (rAAV2) particle assembly using stable producer cell lines. *J Gene Med* **6**: 555–564.

41. Clément, N, Knop, DR and Byrne, BJ (2009). Large-scale adeno-associated viral vector production using a herpesvirus-based system enables manufacturing for clinical studies. *Hum Gene Ther* **20**: 796–806.
42. Chulay, JD, Ye, GJ, Thomas, DL, Knop, DR, Benson, JM, Hutt, JA *et al.* (2011). Preclinical evaluation of a recombinant adeno-associated virus vector expressing human alpha-1 antitrypsin made using a recombinant herpes simplex virus production method. *Hum Gene Ther* **22**: 155–165.
43. Vandenberghe, LH, Xiao, R, Lock, M, Lin, J, Korn, M and Wilson, JM (2010). Efficient serotype-dependent release of functional vector into the culture medium during adeno-associated virus manufacturing. *Hum Gene Ther* **21**: 1251–1257.
44. Smith, RH, Ding, C and Kotin, RM (2003). Serum-free production and column purification of adeno-associated virus type 5. *J Virol Methods* **114**: 115–124.
45. Lock, M, Alvira, M, Vandenberghe, LH, Samanta, A, Toelen, J, Debyser, Z *et al.* (2010). Rapid, simple, and versatile manufacturing of recombinant adeno-associated viral vectors at scale. *Hum Gene Ther* **21**: 1259–1271.
46. Rice, SA and Knipe, DM (1990). Genetic evidence for two distinct transactivation functions of the herpes simplex virus alpha protein ICP27. *J Virol* **64**: 1704–1715.
47. Clark, KR, Voulgaropoulou, F and Johnson, PR (1996). A stable cell line carrying adenovirus-inducible rep and cap genes allows for infectivity titration of adeno-associated virus vectors. *Gene Ther* **3**: 1124–1132.
48. Klein, RL, Meyer, EM, Peel, AL, Zolotukhin, S, Meyers, C, Muzyczka, N *et al.* (1998). Neuron-specific transduction in the rat septohippocampal or nigrostriatal pathway by recombinant adeno-associated virus vectors. *Exp Neurol* **150**: 183–194.
49. Zolotukhin, S, Potter, M, Hauswirth, WW, Guy, J and Muzyczka, N (1996). A "humanized" green fluorescent protein cDNA adapted for high-level expression in mammalian cells. *J Virol* **70**: 4646–4654.
50. Zolotukhin, S, Byrne, BJ, Mason, E, Zolotukhin, I, Potter, M, Chesnut, K *et al.* (1999). Recombinant adeno-associated virus purification using novel methods improves infectious titer and yield. *Gene Ther* **6**: 973–985.
51. Conway, JE (2001). Herpes Simplex Virus Type I based systems for the large scale production of recombinant adeno-associated virus type 2 vectors. College of Medicine, vol. Ph.D. Johns Hopkins University. pp. 184.
52. Falk, DJ, Mah, CS, Soustek, MS, Lee, KZ, Elmallah, MK, Cloutier, DA *et al.* (2013). Intrapleural administration of AAV9 improves neural and cardiorespiratory function in Pompe disease. *Mol Ther* **21**: 1661–1667.